Multivariate signals of population collapse in a high-throughput ecological experiment.

Francesco Cerini[1], John Jackson[1], Dylan Z. Childs[1], and Christopher F. Clements[1]

[1]Affiliation not available

November 20, 2023

Research Article

Multivariate signals of population collapse in a high-throughput ecological experiment.

*Francesco Cerini[1,2], *John Jackson[3,4], Dylan Z. Childs[3], Christopher F. Clements[2]

[1]*Dipartimento Scienze Ecologiche e Biologiche, Università della Tuscia, Viterbo, Italy*

[2]*School of Biological Sciences, University of Bristol, Bristol, UK*

[3]*School of Biosciences, University of Sheffield, Sheffield, UK.*

[4]*Department of Conservation Biology and Global Change. Estación Biológica de Doñana (EBD-CSIC). Avenue Americo Vespucio 26, 41092 Seville, Spain*

Corresponding Author – Francesco Cerini,*francesco.cerini@unitus.it*

* Shared authorship

Author ORCIDs: FC - 0000-0002-1367-1239, JJ - 0000-0002-4563-2840, DZC - 0000-0002-0675-4933, CFC - 0000-0001-5677-5401

Author contribution statement

CC and DC formulated the initial theoretical framework. All authors aided in experimental design. FC performed the experiments. FC and JJ performed data wrangling and analysis. FC and JJ wrote the first draft of the manuscript. All authors contributed equally to the final draft. FC and JJ are both to be considered first authors.

Declaration of Competing Interest

We declare that there are no competing interests.

Data Availability Statement

All code, output and analysis data used in the current study are archived using the Zenodo repository DOI: 10.5281/zenodo.10160252, which was created from the following GitHub repository: https://github.com/jjackson-eco/timeline_demonstration

Abstract

Predicting the future dynamics of populations is a key goal in ecology. Recent conceptual work has suggested that populations under a growing stressor should exhibit a series of stereotypical and sequential shifts in behaviour, traits, and finally abundance before undergoing decline to extinction. This *timeline* of

signals is a promising theoretical framework to forecast population declines in ecological systems long before system/population collapse. However, the need for high-resolution multidimensional data simultaneously characterising, at the individual level, behaviour and traits, as well as population-level measures of abundance, over several generations, has prevented empirical demonstrations of a timeline to collapse. Here, we use an autonomously monitored, high-throughput experimental system to generate individual-based data on populations of the ciliate *Paramecium caudatum* forced to collapse due to increasingly stressful environments. We demonstrate that the gradual introduction of a pollution stressor elicited a predictable sequence of stress responses - declines in movement speed, then body length, then early warning signals of population collapse, and finally abundance declines. Contrarily, a press disturbance generated by introduction of predators did not induce the timeline of signals. The onset of detectable signals of stress in the gradually polluted populations occurred one generation before early warning signals were detectable, and two generation before abundance decline, emphasising that monitoring the behaviours and traits of individuals provides crucial information to help effectively forecast population declines.

Introduction

Human activities are the root cause of stressors including habitat loss and degradation, climatic change, overexploitation, pollutants and the introduction of invasive species (Bonebrake *et al.* 2019; IPBES 2019), which pose both immediate risks of population decline, and future risks of abrupt ecosystem change (Botta *et al.* 2019; Pigot*et al.* 2023). Such abrupt change arises when species can no longer adapt or move in response to stress, resulting in local extinction (i.e. collapse in species abundance), which can destabilise ecological networks and hamper ecosystem service provision (Strona 2022). Given this, our ability to predict whether a given population is at risk of collapse is a fundamental goal in biodiversity monitoring and conservation. Extensive efforts have been made to analyse and forecast population dynamics, either using empirically derived population models to understand extinction risk (e.g. population viability analysis, Chaudhary & Oli 2020; Coulson *et al.* 2001; Jackson*et al.* 2019), or forecasting the occurrence of a critical transitions using early warning signals (EWSs) based on changes in the abundance of a population(Clements & Ozgul 2018). However, such tools are highly variable in their reliability (Brook *et al.* 2000; Butitta *et al.* 2017; Patterson *et al.* 2021; Su *et al.* 2021), particularly when data quality is poor (e.g. time series long enough to capture demographic processes, Coulson *et al.*2001) and model assumptions are not met (Boettiger & Hastings 2012). Most importantly, current tools are often limited in their forecast horizon; the upper limit of time in the future for effectively predicting ecological change (Clements & Ozgul 2016a; Petchey *et al.* 2015). Short forecast horizons hamper our ability to implement management actions and reverse population declines, and increasing the forecast horizon is a key goal in biodiversity monitoring (IPBES 2019).

Recent advances have highlighted the value of incorporating data beyond that typically used in predictive ecology (abundance and demography), particularly individual based data (behaviour and morphology), which are predicted to change rapidly in response to stressors (Cerini *et al.* 2023a; Clements & Ozgul 2018). For example, including body size data in EWS frameworks increases the accuracy of signals inferring collapse and decreases the length of time series required to predict critical transitions (Clements *et al.* 2017; Clements & Ozgul 2016a). Indeed, scaling from individual level processes to the population level, from a basis of physiological responses to the environment (Brown *et al.* 2004; Wikelski & Cooke 2006), can provide a more complete picture of population change (Cerini *et al.* 2023a). For example, environmental stressors influence physiological pathways, which in the short-term can impact behaviour; but over longer timescales chronic stressors influence morphological traits and, ultimately, demographic rates and population dynamics (Guindre-Parker & Rubenstein 2021). Thus, downstream effects of stressor-induced physiological changes acting on behaviour and morphology create the opportunity to observe a sequence of signals before changes in population abundance occur, which we term the*timeline to population collapse* (Cerini *et al.* 2023a) or simply *timeline to collapse* . The timeline to collapse, integrating individual and population level responses to stressors, lays the conceptual groundwork for a generalizable framework in ecological monitoring, with far-reaching potential to improve the forecast horizon and the reliability of EWSs.

The implementation of the timeline to collapse framework requires intensive monitoring of populations

to build time series of multidimensional data from the individual to the population level (e.g. behaviour, morphology and abundance, Cerini *et al.* 2023a). Promisingly, the rise of autonomous monitoring in ecology has the potential to fill this multidimensional data gap (Besson *et al.*2022; Cavender-Bares *et al.* 2022), but in spite of this, an appropriate dataset to empirically test the timeline has previously not existed. Here we employ a cutting-edge autonomous monitoring system to collect multidimensional data on experimental protist populations that were driven to extinction by increasingly stressful environmental conditions. The conceptual framework assumes that a gradual increase from low to high stressors levels (i.e. ramp disturbance (Lake 2003)) is the ideal condition to observe the timeline of signals, whereby individuals have time to implement phenotypical responses (Cerini*et al.* 2023a). In contrast, an immediate transition from unstressed to stressed conditions, characterized by a sudden, high-magnitude stressor event (i.e. a press disturbance, Bender *et al.* 1984) might be less likely to generate an observable timeline to collapse. Thus, to test both scenarios, we induced decline in populations of the widely used ciliate model *Paramecium caudatum*by means of: i) gradually increasing the levels of a pollutant (ramp disturbance), and ii) the introduction of a predatory species (press disturbance), whilst concurrently monitoring movement speed, body size, and abundance nine times every generation. We compared control and stressor treatments using general additive models and predicted the temporal occurrence of changes in behaviour, morphology, abundance trends, and widely used abundance EWSs. We show that the pollution stressor induced a clear series of observable changes which mirrored that predicted by the timeline to collapse conceptual model, where shifts in the individual-level features (behaviours, morphologies) were detected more than two generation times before the abundance decline to extinction. However, due to the sudden occurrence of high predation rates, the timeline was not observed in populations stressed by the addition of a predator, confirming that its occurrence might depend on stressor typology and severity.

Results

We established 10 replicate populations of *P. caudatum* for each of three experimental treatments: control, increasing Cu^{2+} pollution, and introduction of a*Stenostomum virginianum* flatworm predator population (Figure 1). Following five days of initial acclimatisation in the absence of any stressor, populations were monitored for a total of approximately 24 generations, with the full experiment lasting 560 hours. We introduced stressors after ˜330 hours (14 generations). We monitored populations using a robotic-gantry mounted camera, which recorded 12 seconds of video for each population every three hours. We then extracted individual and population level data from each video using the open-source ComTrack machine-learning algorithm (Besson *et al.* 2021). We monitored the mean movement speed (behaviour, mm s^{-1}; Figure 1a), mean body length (morphology, µm; Figure 1b), and maximum video-derived abundance (number of individuals; Figure 1c) at each time point. Daily cycles of *P. caudatum* abundances due to disturbance (see Methods) were removed with seasonal decomposition by loess (Fig. S1-3). We observed some variability among the replicates of control populations, with one undergoing collapse spontaneously, and three replicates gaining higher densities compared to the remaining five, which were similar in their abundance trends (Figure 1). All polluted populations underwent collapse after approximately five generations from the initial introduction of the stressor (Figure 1). In two of the predator treatment populations, the flatworm did not cause collapse (Figure 1). These two predator replicates and the collapsing control replicate were excluded from the analysis (final N = 27).

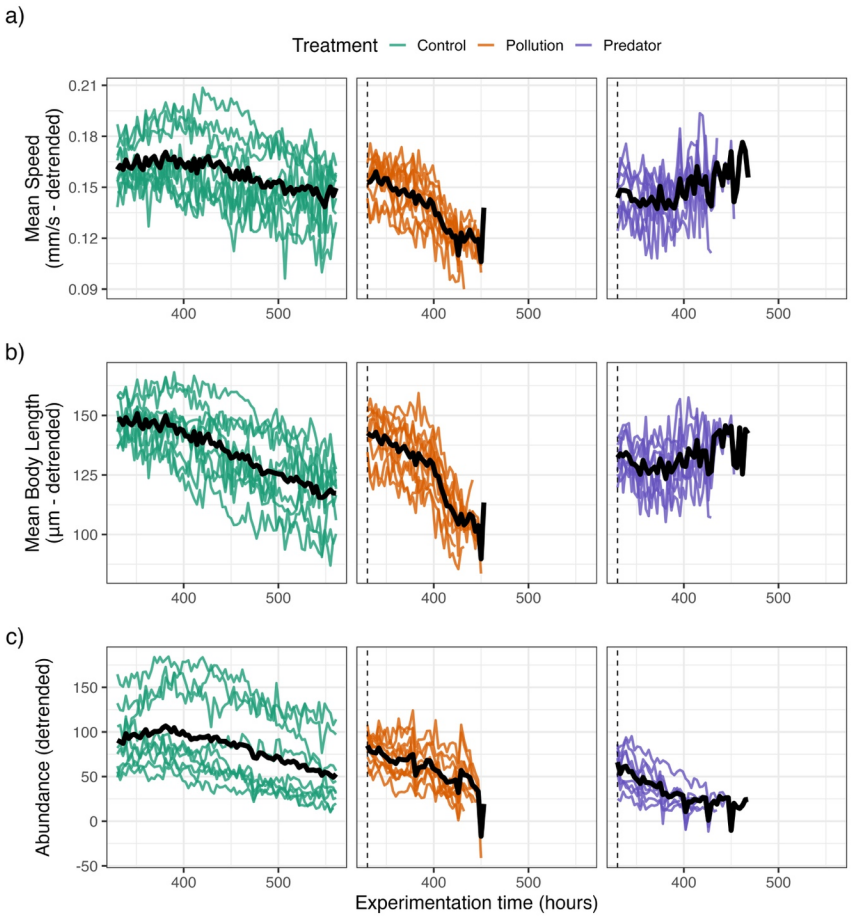

Figure 1. Detrended time series of the tracked P. caudatum mean swimming speeds (a), body lengths (b) and number of individuals (c) in the three treatments (Green-Control, Orange-Pollution, Purple-Predator). Coloured lines represent the single replicates. The thick black line is mean between replicates. The dashed vertical line marks the start of the stressors.

We found evidence for a timeline to collapse in the pollution treatment, which increased the forecast horizon relative to EWS analysis (Figure 2). We assessed the presence of a sequence of signals indicating collapse using mean generalised additive model predictions for the temporal trend in each variable, and assessed divergence between trends using deviation in 95% confidence intervals derived using posterior simulation (Figure 2). For the pollution treatments, mean movement speed significant reduced after 3.18 generations from the start of the stressor (73 hours [65; 78], upper and lower confidence limits of split point based on posterior resampling), when compared to the control treatments (Figure 2a). Then, 3.96 generations (91 hours [88; 103]) after the beginning of the pollution, and 0.8 generations (18 hours) after the behavioural change, the mean body length displayed a detectable decline compared to the control (Figure 2b). Finally, 4.83 generations (111 hours [98; 114]) after introducing pollution, and 1.65 generations (38 hours) after the morphology signal, the abundance trend diverged significantly from the control. The predicted abundance trend reached the point of collapse at time point 451, that is, the pollution brought the population to functional extinction after 5.34 generations, and the behavioural and morphological shifts preceded the collapse of respectively 2.1 and 1.3 generations. We also assessed temporal trends in EWS metrics (coefficient of variation - CV, standard deviation - SD, and lag-1 autocorrelation - ACF; Figure S4) of abundance, normalising the temporal component for each replicate using the time before collapse (time before experiment

end for control treatments). The EWS analysis revealed a significant divergence in CV 1.13 generations (26 hours) before the collapse point, but after changes in both the behaviour and morphology. Critically, the introduction of behavioural and morphological data increased the forecast horizon of population collapse by one generation relative to the EWS analysis. Finally, the observed split points were robust to posterior resampling of predicted temporal trends, displaying a consistent sequence of change in behaviour, morphology and abundance (precluded by an increase in abundance CV) (Figure 2).

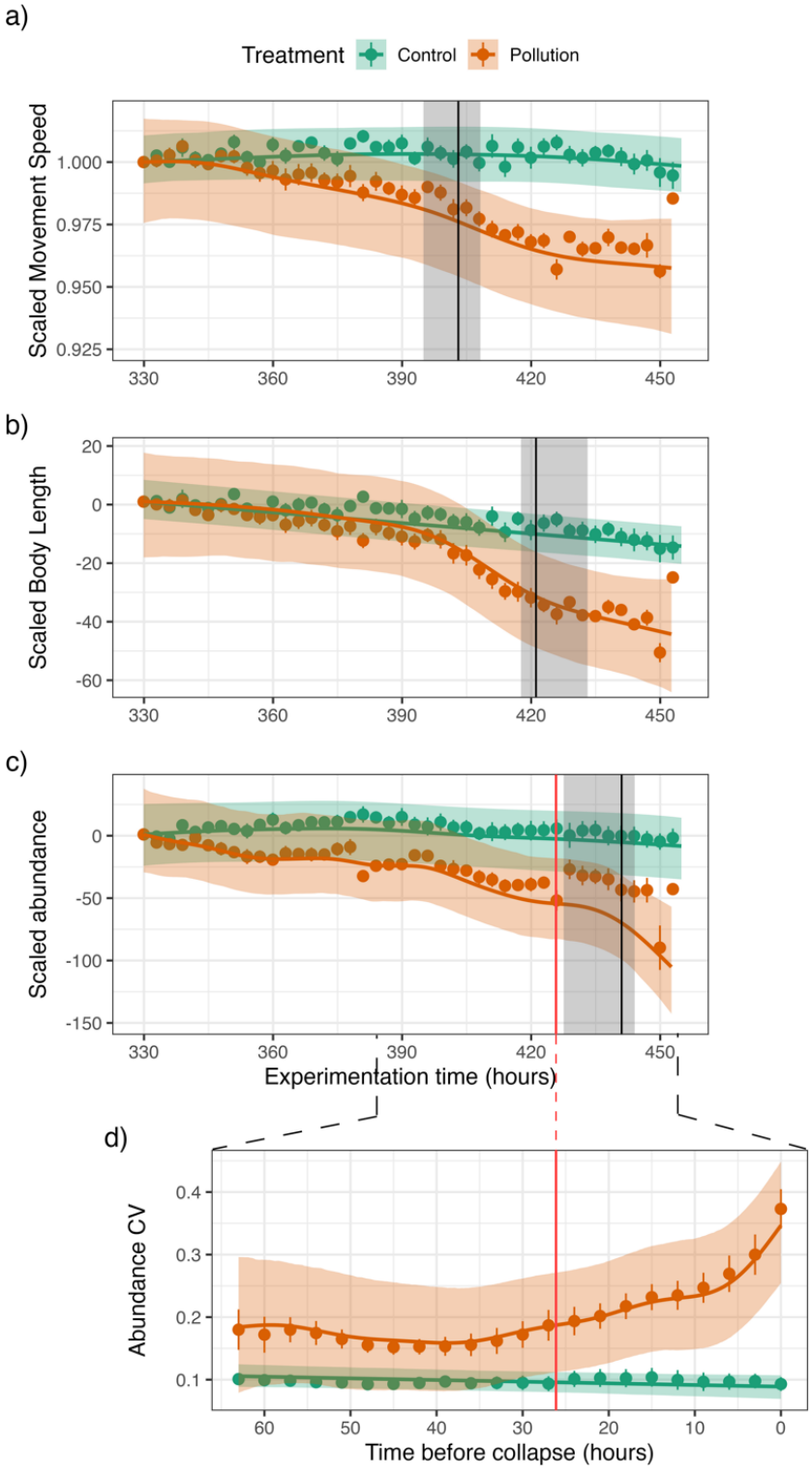

Figure 2. Observed timeline to collapse for the pollution treatment. Detrended and scaled time series of

mean swimming speeds (a), mean body lengths (b), abundance (c) and coefficient of variation (cv, zoomed panel d) starting from the beginning of the stressor treatment (time point 330). The cv is calculated on 50% of the abundance time series and the x axis is converted into hours before collapse to normalize the temporal component for each replicate (i.e. all replicates time series stopping at the same time point)(d). Elements in orange represent the pollution treatment, green elements the control treatment. Points with brackets represent across-replicate mean and standard errors. Continuous lines and shaded areas represent each GAMMS's predicted mean trends with 95% confidence intervals. (a-c) For analysis, predicted timeseries of control and pollution treatments were scaled linearly to begin at a value of 1 when the stressor was introduced. Vertical black lines and relative shaded areas indicate the splitting time point of the confidence interval trends between the two treatments (a significant change compared to the control) with a posterior resampling interval. Red vertical line indicates the occurrence of EWS (significant split in the cv), also projected on the abundance panel.

In contrast to the pollution treatment, the introduction of the flatworm predator was not followed by sequential changes in behaviour, morphology and abundance (Figure 3). Instead, the abundance of the predator treatment began declining immediately following the introduction of the stressor, with a significant deviation in predicted abundance after 72 hours [64;78] or 3.14 generations (Figure 3c). We found no clear trends of deviation in mean speed and body length across the stressor experiment (Figure 3a & 3b). We do not display any split point for mean speed or body length as the confidence intervals resulting overlapped for the entire time series. Finally, the EWS analysis did not show clear patterns in the predator treatment; the coefficient of variation was highly variable and displayed an increasing trend deviating significantly from the control since the addition of predators (Figure S4).

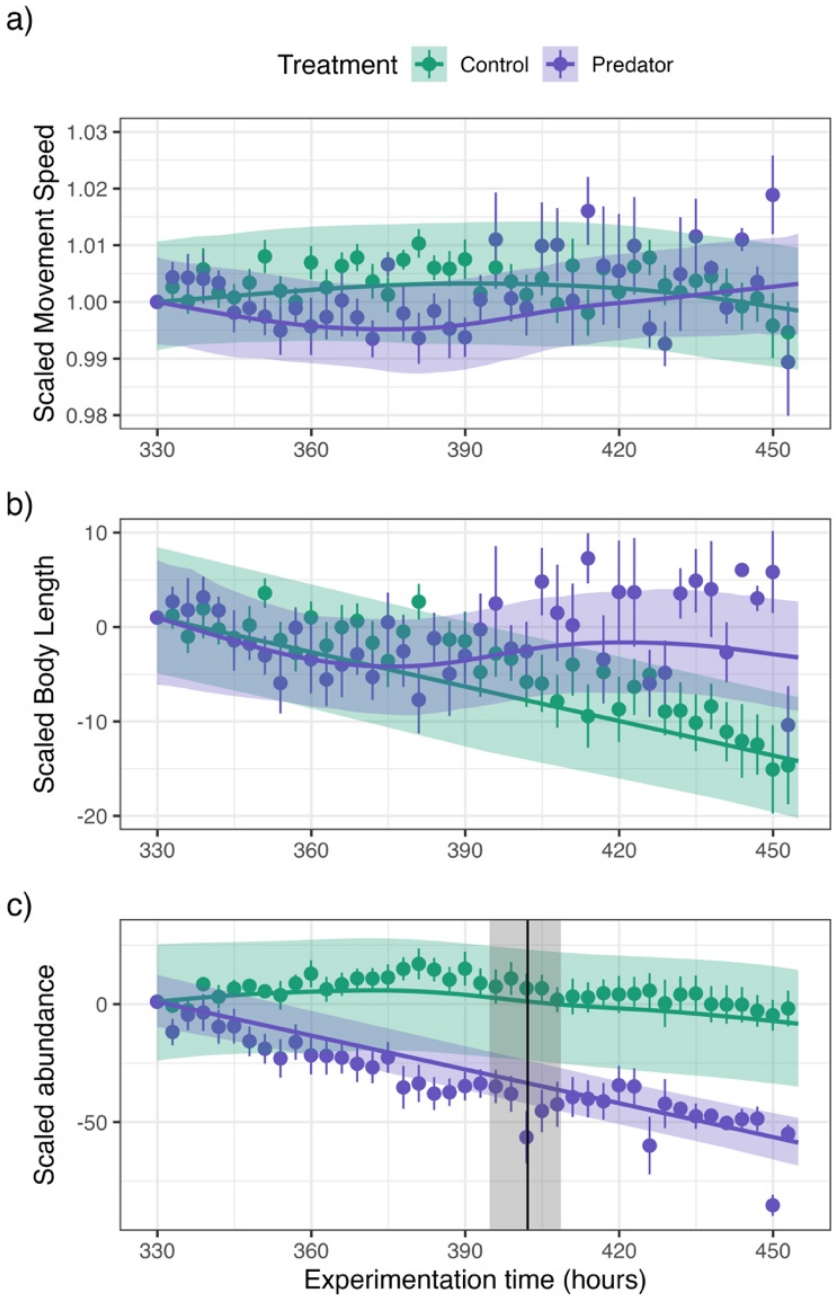

Figure 3. Detrended time series of mean swimming speeds (a), mean body lengths (b) and abundance (c) starting from the beginning of the stressor treatment. Elements in purple represent the predator treatment, green elements the control treatment. Points with brackets represent across-replicate means and standard errors. Continuous lines and shaded areas represent the GAMMs predicted mean trends with 95% confidence intervals. (a-c) For analysis, predicted timeseries of control and pollution treatments were scaled linearly to begin at a value of 1 when the stressor was introduced. Vertical black lines and relative shaded areas indicate the splitting time point of the confidence interval trends between the two treatments (a significant change compared to the control) with a posterior resampling interval.

Discussion

The rapid pace of change in the natural environment is altering the resilience of wild populations (Capdevila *et al.* 2022), with signals of resilience loss (i.e. early warning signals) poised as a crucial tool for biodiversity management and protection (Nijp *et al.* 2019; Stelzer *et al.* 2021). However the application of these methods is currently hampered by their reliability and their limited forecast horizon (Baruah *et al.* 2020; Patterson *et al.*2021). Expanding these predictive frameworks to include information at the individual level gives rise to potentially powerful approaches to forecast population collapse (Clements *et al.* 2017; Clements & Ozgul 2016a). Here, using a novel autonomous, high through-put monitoring system allowing us to track individual behaviour, morphology and population abundance over 24 generations, we find direct experimental evidence to support the conceptual model of a timeline to population collapse (Cerini *et al.* 2023a). Namely, we find a sequential shift in behaviour, then morphology, and finally abundance in response to a gradually increasing environmental stressor. Such signals were detectable up to 1.65 generations before a significant decrease in abundance, and crucially a whole generation before a detectible early warning signal. The successive changes from the individual to the population level represented a growing body of evidence, strengthening the inference of an approaching collapse. However, the occurrence of the timeline to collapse seems to be partly dependant on the stressor nature. We highlight that integrative ecological monitoring approaches, with an emphasis on individual behavioural and morphological data in addition to population monitoring, may represent a crucial next step to forecast population declines more effectively.

The environmental pollution stressor generated a clear timeline of changes matching the theoretical framework (Cerini *et al.* 2023a). Generally, changes in the behavioural spectrum are among the earliest and commonest responses to environmental change. Stress-induced behavioural change can take the form of shifts in activity patterns, distributional range or ecological choices (e.g. antipredatory behaviours, foraging, nesting or reproductive preferences, Berger-Tal*et al.* 2011; Rabaiotti & Woodroffe 2019). In our experiment, the behavioural shift preceded the morphological shift by nearly a whole generation, indicating that the locomotory system of *P. caudatum*was the first to be affected by the pollutant. Copper ions are known to affect the food vacuole forming capacity and chemotaxis in ciliates (Dale 1991; Nilsson 1981). Thus, the observed decrease in movement speed was likely due to a general energy availability reduction for the*P. caudatum* cells, as their food intake system was compromised. Often behavioural traits are more plastic than other features (e.g. life history, Refsnider & Janzen 2012), and can buffer organisms against resource reduction (Goossens *et al.* 2020) or temperature change (Chen *et al.* 2011). After the shift in cell movement could not avert a physiological change, there was a reduction in food intake affecting *P. caudatum* morphology. The timing between shifts in individual traits will vary between species, but a behavioural change may occur up to and over a generation before morphological change. For example, food resource reduction increases the foraging distance in seabirds (Fayet *et al.* 2021). In this case, we might observe a longer time gap before the morphology and demography are affected. Ultimately however, characterising individual phenotypic traits can add important insights into population decline (Cerini *et al.* 2023a).

The next observed signal in the timeline was the shift in morphology. Change in morphological features is a general physiological response to energy intake reduction (e.g. mass reduction), but also to other kinds of stressors (e.g. environmental warming, Sheridan & Bickford 2011), including predator presence (Chiba 2007). The mean *P. caudatum*length declined strongly before the trend nearly plateaued over an approximate two-generation time interval (Figure 2). At that point, most individuals were not able to reproduce and function anymore, and the population abundance started to decrease. Generally, the observation of a morphological shift after a behaviour change should be considered as a pivotal moment in view of management of vulnerable populations, as it is the last signal observable before stressors act directly on the survival of individuals (i.e. affecting the population dynamics, Cerini *et al.* 2023a). Indeed, for larger organisms such as vertebrates, the capacity of body size to change for long periods of time (e.g. polar bears weight loss, Stirling & Derocher 2012) as reaction to stressors provides an opportunity to perform conservation actions.

After the morphological change, the populations showed a rapid decline to collapse in little more than one generation. Before collapse, we observed a potential EWS: an increase in the coefficient of variation

of abundance, diverging from the control approximately one generation before collapse. Thus, it might represent a final measurable signal in the timeline before the decline in abundance, becoming visible after the behavioural and morphological change. The coefficient of variation proved to be a useful EWS forecasting abrupt changes in other systems (Clements & Ozgul 2018). However, the coefficient of variation was one indicator out of three tested (see Supplementary Material), and EWS metrics are prone to indicate false positives (Boettiger & Hastings 2012; Patterson *et al.* 2021), and thus solely relying on EWS metrics may not be a reliable. Indeed, the forecast horizon of the EWS (˜one generation) is a half compared to the first behavioural signal and is likely not sufficient for meaningful action in a real-world conservation scenario. Hence, the observation of the timeline signals before the EWS builds not only a wider forecast horizon, but also acts as a quality check for classic resilience loss indicators. By confirming that they are actually representing the systematic loss of resilience as a tipping point is approached, the timeline framework can help in reducing the false positive rates of classic EWS.

In contrast to the pollution treatment, the predator introduction, a press disturbance scenario, did not result in the predicted sequence of observable signals prior to a populations collapse. Whilst ciliates, and the *Paramecium* genus in particular, are known to display antipredatory behavioural and morphological responses(Cerini *et al.* 2023b; Fyda *et al.* 2005), neither behavioural nor morphological traits showed a clear pattern of change compared to the control in the predator treatment. Exposure to predatory *Stenostomum* cues induced a swimming speed reduction in *Paramecium* , and a cell shape change towards a ball-shape morph (to decrease likelihood of being engulfed by the predator, Hammill*et al.* 2010b). Our lack of observation of similar response may be a function of the predation pressure being too high, and the size of the habitats too small, for the *P. caudatum* individuals to escape or implement antipredatory responses. Thus, predation had an immediate impact on the abundances of the ciliate populations, potentially reducing the opportunity to elicit measurable behavioural or morphological change. Such contrast between responses to predators and pollution supports previous work suggesting that rapid onset of high intensity stressors (e.g. extreme events) can prevent meaningful forecasting in wildlife populations (Clements & Ozgul 2016b), and suggests that ramp disturbances (environmental pollution, temperature increase, habitat loss) as the best suited scenario for the timeline application. Additionally, this suggests that the observation of the timeline to collapse will depend on the mechanisms by which the stressor acts on the population.

Adapting the observed timeline to collapse for wildlife conservation is non-trivial, mostly given the lack of standard controls with which compare the observed trends and thus to infer the occurrence of sequential signal (as we did using the GAMM predictions). The use of historical thresholds (Donadio Linares 2022) or comparisons with non-stressed population (space-per-time substitution, Fayet *et al.* 2021) can help in pinpointing deviations in the behavioural or morphological traits. However, concurrent monitoring of individual traits and abundance has the potential to increase the time window available to implement management actions, and thus developing frameworks to leverage multidimensional data remains a priority. Following our experimental example, after the observation of the first behavioural signal one could have stopped the pollution (i.e. cutting a chemical waste from an ecosystem, Vorobeichik 2022) avoiding critical levels. More experiments are needed to both increase the spectrum of tested stressors and the complexity of the taxa, and mesocosm experiments with multicellular organism are the obvious next step to improve the generalizability of the framework. Nevertheless, we urge ecologists to take advantage of autonomous monitoring tools for biodiversity monitoring (Besson *et al.* 2022; Cavender-Bares*et al.* 2022), which can collect multidimensional data to more effectively predict population change (Cerini *et al.* 2023a).

In conclusion, our results demonstrate a timeline of signals preceding population collapse (Cerini *et al.* 2023a), which can improve the forecast horizon of early warning signals. A pollution stressor represents a clear case where the individual traits displayed shifts more than two generations before a decline in abundance. Additionally, the observation of the sequence of signals indicates that as the stressor is increasing, different dimensions of a population are being engaged, thus highlighting the adaptability of the population to new conditions.

Methods

Experimental protocol

A stock of *Paramecium caudatum,* kept at Bristol University and originally purchased from Sciento (Manchester, UK), was raised in a temperature-controlled room for two weeks at 18°C and 80% humidity in constant light environment. The growth medium consisted of crushed protozoa pellets (Blades Biological LTD) dissolved in Chalkley's solution at a concentration of 0.3 $g.L^{-1}$, then autoclaved (Clements *et al.* 2013). The medium was then filtered through Whatman no.1 filter paper to improve media clarity and autoclaved again. This medium was inoculated with two species of bacteria, *Bacillus subtilis* and *Pseudomonas fluorescens* . At this conditions *P. caudatum* showed a generation time of ˜ 23 hours.

The experiment was performed in experimental microcosms consisting of rectangular patches (5.6 x 3.6 x 1.6 cm), custom designed using FreeCAD 3D-design software (https://www.freecad.org/) and 3D-printed in clear PLA filament (Lulzbot TAZ 6). The base of each microcosm was painted with black acrylic paint and coated in transparent epoxy resin to smooth the patch surface and prevent potential paint leaching. Each microcosm was filled with 6 ml of the same medium described above, which was inoculated 48h before the start of the experiment. ˜ 60 *P. caudatum* individuals was put in each microcosm and left to grow and reach a stable phase for two weeks. Microcosm were topped up to replace evaporation with autoclaved distilled water every day. At the start of the third week, the stressor treatments were implemented. We had 10 replicates for each treatment for a total of 30 patches. The treatments consisted of: 1) Control treatment: no stressor was applied to the population; 2) Pollution treatment: an increasing quantity of a copper sulphate solution was added everyday over a 10-day period. Copper ions are very toxic for aquatic ciliates (Madoni & Romeo 2006) and have been previously used for experimental extinction tests (Sommer *et al.* 2017). The initial pollution quantity was calculated to reach in the experimental patch 5% of a pre-tested copper concentration (0.6 mgL^{-1}), lethal to a dense population of *P.caudatum.* Every day the quantity was increased, adding the same amount (the initial quantity, 1.5 µl of the copper sulphate solution) to the previous day quantity (i.e. 1.5 µl, 3 µl, 4.5 µl etc); 3) Predator treatment: five individuals of the flatworm *Stenostomum virginianum* were added to each patch. *S. virginianum* is a voracious generalist predator known to prey on most ciliates species (Hammill *et al.* 2010a; Núñez-Ortiz *et al.* 2022). Preliminary tests showed that five individuals were enough to bring a population to extinction over a week.

The microcosms were monitored once every three hours (˜ eight times per generation) for four weeks. The monitoring was performed by means of an automated system consisting of a camera (GXCAM HighChrome-HR4 HI RES) connected to a stereomicroscope (Nikon SMZ1270) attached to a robotic gantry (igus drylin Gantry) programmed to record 12-second videos of each microcosm every three hours. All recorded videos were processed using ComTrack, an open-source machine learning-based software designed to extract individual morphological and behavioural information, as well as species abundances and spatial distributions of individuals from videos(Besson *et al.* 2021).

Data processing

The software outputs were processed using R (version 4.3.1, R Core Team 2022) to extract information on the speed and body length of every tracked individual of *P. caudatum* (Supplementary Material), and the total number of individuals tracked (abundance) at every time point. From our raw dataset we calculated the mean speed – as an indicator of behaviour (Hammill *et al.* 2010a) – and mean length – as a plastic morphological feature subject to variation in response to stressors (Uiterwaal *et al.* 2020) – of every individual in each of the 12 second videos. Thus, across all the treatments and replicates, each tracked ciliate had a mean value of speed and length for each sampling point. For analysis, we averaged speed and body length values across all individuals and frames in each time point, resulting in a single feature value for each population per time point (Supplementary Material Fig. S1). On visual inspection, we found that the data were displaying a regular daily cycle of values, most evident in the abundance time series (Supplementary Material Fig. S1A). This occurred due to the daily topping up of each population with distilled water to maintain the initial volume: the perturbation of the microcosm (addition of the water) induced a sudden increase in movement and activity, and many of the non-moving protists (not tracked in stable conditions) would become trackable, thus increasing the abundance counts. Due to the daily regularity of these spikes, we removed daily cycles

in raw data using the additive seasonal decomposition by loess (STL, Cleveland *et al.* 1990). In the STL decomposition, we extracted seasonal components with a cycle of 8 observations, and a trend resolution of 20 observations. We subtracted the resulting seasonal time-series from the raw data, resulting in a de-cycled timeseries with trend and anomaly components.

Time series analysis

We captured the temporal change in speed, length and abundance using the de-cycled data (Fig. 1) and focused the analysis on the interval between the onset of the stressors (330 hours after the beginning of the experiment) and the endpoint of the experiment (550 hours, Fig.1). One replicate of the control treatment collapsed for unknown reasons and thus was not considered, as well as the two replicates of the predator treatment that did not undergo collapse. Each time series in the stressor treatments was defined as collapsed at the time point when the abundance fell below 10% (Aagaard *et al.* 2016) of the abundance after 10 days of growth and acclimation. We then fitted generalized additive mixed models (GAMM) on the resulting time series with the response variables of mean speed, mean length, and abundance of the populations across the three treatments (control, pollution, predator), resulting in nine statistical models. GAMMs were fit using the*mgcv* package (Wood 2011). The general form of the model was as follows, where the mean timeline response variable, τ, for row$i$ and replicate r,

$$\tau_{i,r} = \beta^0 + f_t(T_i) + f_R(T_{i,r}) + f_e(R_r) + f_a(G_i),$$

Where β^0 is the global intercept. The term$f_t(T_i)$ is the key overall predictor of time point (T), for which the smoothing function f_t was fit with a thin plate regression spline (Wood 2003). The basis dimension of$f_t(T_i)$ for each response variable was determined using AIC model selection for a range of k values (Supplementary Material). We also included $f_R(T_{i,r})$, which gives individual time-point smoothing terms for each replicate population, to account for the variability in temporal patterns between replicates following(Pedersen *et al.* 2019). We fit a general random effect term, $f_e(R_r)$, for replicate population (R), to account for intercept differences between replicates(Wood 2017). Separately, we explored patterns of temporal autocorrelation in each of the time-series using partial autocorrelation, and determined that lag-1 autocorrelation terms were sufficient in each of the three response variables (Supplementary Material). Therefore, we also included the term $f_a(G_i)$, where G gives the time point expressed as a categorical factor, and the function f_a gives a lag-1 autocorrelation structure fit using the *nlme* package in R(Pinheiro *et al.* 2017). All models were fit with a Gaussian distribution.

Early warning signals

To assess if the collapse of the populations could be preceded by generic early warning signals, we used the R package *EWSmethods* (O'Brien *et al.* 2022) to extract time series of the standard deviation, coefficient of variation, and autocorrelation for each replicate of each treatment, calculated with a rolling window approach using 50% of each replicate time series. We then fitted GAMMSs on the time series of such indicators. The GAMMSs had the same structure described above. However, to improve comparability among replicates for EWS metrics, we modified the independent variable of time point to represent the hours before collapse, thus every replicate EWS would end in the same time point (0).

Pinpointing the timeline signals

We assessed the time-points at which control and treatments diverged for each of the multi-dimensional timeseries, and thus the presence of the timeline to collapse signals, using a predictive simulation framework. We calculated predictions using posterior simulations of each model, using 500 unique time-point values between the start of the stressors and the end of the experiment. Posterior predictions included only the overall time-point smoothing term, averaging all additional variation between replicates. Thus, predictions are for the mean temporal trend effect. For analysis, control and treatment predicted timeseries were scaled linearly so that predicted values were 1 at the introduction of the stressor. We assessed the 95% confidence intervals, which we used to determine the divergence points, using posterior simulation. We sampled 1000

unique values of each model coefficient under parameter uncertainty using a multivariate normal distribution (implemented in the *MASS* package ,Venables & Ripley 2002). We combined simulated model coefficients with the linear prediction matrix to retrieve 1000 sets of predicted values, from which we ascertained the upper and lower 95% confidence limits of the temporal trend. Then, the divergence point between control and treatment predictions was the last point at which the confidence limit of the control overlapped with the treatment prediction, that is, the time point where the difference between the upper and lower confidence intervals of control and treatment reached 0. Finally, we assessed the sensitivity of the divergence points to the posterior resampling, in which we re-sampled 10% of the prediction data and recalculated 100 divergence points, to give confidence limits in divergence.

References

Aagaard, K., Lockwood, J.L. & Green, E.J. (2016). A Bayesian approach for characterizing uncertainty in declaring a population collapse.*Ecological Modelling* , 328, 78–84.

Baruah, G., Clements, C.F. & Ozgul, A. (2020). Eco-evolutionary processes underlying early warning signals of population declines.*Journal of Animal Ecology* , 89, 436–448.

Bender, E.A., Case, T.J. & Gilpin, M.E. (1984). Perturbation Experiments in Community Ecology: Theory and Practice. *Ecology* , 65, 1–13.

Berger-Tal, O., Polak, T., Oron, A., Lubin, Y., Kotler, B.P. & Saltz, D. (2011). Integrating animal behavior and conservation biology: a conceptual framework. *Behavioral Ecology* , 22, 236–239.

Besson, M., Alison, J., Bjerge, K., Gorochowski, T.E., Høye, T.T., Jucker, T., *et al.* (2022). Towards the fully automated monitoring of ecological communities. *Ecology Letters* .

Besson, M., Gilliot, P.-A.M.A., Gorochowski, T.E. & Clements, C.F. (2021). Automated tracking and species classification of ecological communities. Presented at the Ecology across borders 2021.

Boettiger, C. & Hastings, A. (2012). Quantifying limits to detection of early warning for critical transitions. *Journal of The Royal Society Interface* , 9, 2527–2539.

Bonebrake, T.C., Guo, F., Dingle, C., Baker, D.M., Kitching, R.L. & Ashton, L.A. (2019). Integrating Proximal and Horizon Threats to Biodiversity for Conservation. *Trends in Ecology & Evolution* , 34, 781–788.

Botta, F., Dahl-Jensen, D., Rahbek, C., Svensson, A. & Nogués-Bravo, D. (2019). Abrupt Change in Climate and Biotic Systems. *Current Biology* , 29, R1045–R1054.

Brook, B.W., O'Grady, J.J., Chapman, A.P., Burgman, M.A., Akçakaya, H.R. & Frankham, R. (2000). Predictive accuracy of population viability analysis in conservation biology. *Nature* , 404, 385–387.

Brown, J.H., Gillooly, J.F., Allen, A.P., Savage, V.M. & West, G.B. (2004). Toward a Metabolic Theory of Ecology. *Ecology* , 85, 1771–1789.

Butitta, V.L., Carpenter, S.R., Loken, L.C., Pace, M.L. & Stanley, E.H. (2017). Spatial early warning signals in a lake manipulation.*Ecosphere* , 8, e01941.

Capdevila, P., Noviello, N., McRae, L., Freeman, R. & Clements, C.F. (2022). Global patterns of resilience decline in vertebrate populations.*Ecology Letters* , 25, 240–251.

Cavender-Bares, J., Schneider, F.D., Santos, M.J., Armstrong, A., Carnaval, A., Dahlin, K.M., *et al.* (2022). Integrating remote sensing with ecology and evolution to advance biodiversity conservation.*Nat Ecol Evol* , 6, 506–519.

Cerini, F., Childs, D.Z. & Clements, C.F. (2023a). A predictive timeline of wildlife population collapse. *Nat Ecol Evol* , 7, 320–331.

Cerini, F., O'Brien, D., Wolfe, E., Besson, M. & Clements, C.F. (2023b). Phenotypic response to different predator strategies can be mediated by temperature. *Ecology and Evolution* , 13, e10474.

Chaudhary, V. & Oli, M.K. (2020). A critical appraisal of population viability analysis. *Conservation Biology* , 34, 26–40.

Chen, I.-C., Hill, J.K., Ohlemüller, R., Roy, D.B. & Thomas, C.D. (2011). Rapid Range Shifts of Species Associated with High Levels of Climate Warming. *Science* , 333, 1024–1026.

Chiba, S. (2007). Morphological and ecological shifts in a land snail caused by the impact of an introduced predator. *Ecol Res* , 22, 884–891.

Clements, C.F., Blanchard, J.L., Nash, K.L., Hindell, M.A. & Ozgul, A. (2017). Body size shifts and early warning signals precede the historic collapse of whale stocks. *Nat Ecol Evol* , 1, 0188.

Clements, C.F. & Ozgul, A. (2016a). Including trait-based early warning signals helps predict population collapse. *Nat Commun* , 7, 10984.

Clements, C.F. & Ozgul, A. (2016b). Rate of forcing and the forecastability of critical transitions. *Ecology and Evolution* , 6, 7787–7793.

Clements, C.F. & Ozgul, A. (2018). Indicators of transitions in biological systems. *Ecol Lett* , 21, 905–919.

Clements, C.F., Warren, P.H., Collen, B., Blackburn, T., Worsfold, N. & Petchey, O. (2013). Interactions between assembly order and temperature can alter both short- and long-term community composition. *Ecol Evol* , 3, 5201–5208.

Cleveland, R.B., Cleveland, W.S., McRae, J.E. & Terpenning, I. (1990). STL: A seasonal-trend decomposition.

Coulson, T., Mace, G.M., Hudson, E. & Possingham, H. (2001). The use and abuse of population viability analysis. *Trends in Ecology & Evolution* , 16, 219–221.

Dale, T. (1991). Protists and Pollution — with an Emphasis on Planktonic Ciliates and Heavy Metals. In: *Protozoa and Their Role in Marine Processes* (eds. Reid, P.C., Turley, C.M. & Burkill, P.H.). Springer Berlin Heidelberg, Berlin, Heidelberg, pp. 115–130.

Donadio Linares, L.M. (2022). The awkward question: What baseline should be used to measure biodiversity loss? The role of history, biology and politics in setting up an objective and fair baseline for the international biodiversity regime. *Environmental Science & Policy* , 135, 137–146.

Fayet, A.L., Clucas, G.V., Anker-Nilssen, T., Syposz, M. & Hansen, E.S. (2021). Local prey shortages drive foraging costs and breeding success in a declining seabird, the Atlantic puffin. *J Anim Ecol* , 1365-2656.13442.

Fyda, J., Warren, A. & Wolinńska, J. (2005). An investigation of predator-induced defence responses in ciliated protozoa. *Journal of Natural History* , 39, 1431–1442.

Goossens, S., Wybouw, N., Van Leeuwen, T. & Bonte, D. (2020). The physiology of movement. *Mov Ecol* , 8, 5.

Guindre-Parker, S. & Rubenstein, D.R. (2021). Long-Term Measures of Climate Unpredictability Shape the Avian Endocrine Stress Axis.*The American Naturalist* , 198, 394–405.

Hammill, E., Kratina, P., Beckerman, A.P. & Anholt, B.R. (2010a). Precise time interactions between behavioural and morphological defences. *Oikos* , 119, 494–499.

Hammill, E., Petchey, O.L. & Anholt, B.R. (2010b). Predator Functional Response Changed by Induced Defenses in Prey. *The American Naturalist* , 176, 723–731.

IPBES. (2019). *Global assessment report on biodiversity and ecosystem services of the Intergovernmental Science-Policy Platform on Biodiversity and Ecosystem Services* . Zenodo.

Jackson, J., Childs, D.Z., Mar, K.U., Htut, W. & Lummaa, V. (2019). Long-term trends in wild-capture and population dynamics point to an uncertain future for captive elephants. *Proc. R. Soc. B.* , 286, 20182810.

Lake, P.S. (2003). Ecological effects of perturbation by drought in flowing waters. *Freshwater Biology* , 48, 1161–1172.

Madoni, P. & Romeo, M.G. (2006). Acute toxicity of heavy metals towards freshwater ciliated protists. *Environmental Pollution* , 141, 1–7.

Nijp, J.J., Temme, A.J.A.M., van Voorn, G.A.K., Kooistra, L., Hengeveld, G.M., Soons, M.B., *et al.* (2019). Spatial early warning signals for impending regime shifts: A practical framework for application in real-world landscapes. *Global Change Biology* , 25, 1905–1921.

Nilsson, J.R. (1981). Effects of copper on phagocytosis inTetrahymena.*Protoplasma* , 109, 359–370.

Núñez-Ortiz, A.R., Nandini, S. & Sarma, S.S.S. (2022). Prey preference of Stenostomum cf. virginianum Nuttycombe, 1931 (Platyhelminthes); a case study in the littoral zone of a tropical reservoir.*Ecohydrology & Hydrobiology* , 22, 168–177.

O'Brien, D., Deb, S., Sidheekh, S., Krishnan, N., Dutta, P.S. & Palakkad, I.I.T. (2022). EWSmethods: an R package to forecast tipping points at the community level using early warning signals and machine learning models.

Patterson, A.C., Strang, A.G. & Abbott, K.C. (2021). When and Where We Can Expect to See Early Warning Signals in Multispecies Systems Approaching Tipping Points: Insights from Theory. *The American Naturalist* , E000–E000.

Pedersen, E.J., Miller, D.L., Simpson, G.L. & Ross, N. (2019). Hierarchical generalized additive models in ecology: an introduction with mgcv. *PeerJ* , 7, e6876.

Petchey, O.L., Pontarp, M., Massie, T.M., Kéfi, S., Ozgul, A., Weilenmann, M., *et al.* (2015). The ecological forecast horizon, and examples of its uses and determinants. *Ecology Letters* , 18, 597–611.

Pigot, A.L., Merow, C., Wilson, A. & Trisos, C.H. (2023). Abrupt expansion of climate change risks for species globally. *Nat Ecol Evol* , 7, 1060–1071.

Pinheiro, J., Bates, D., DebRoy, S., Sarkar, D., Heisterkamp, S., Van Willigen, B., *et al.* (2017). Package 'nlme'. Linear and nonlinear mixed effects models. Available at https://cran.r-project.org/web/packages/nlme/nlme.pdf.

R Core Team. (2022). R: A language and environment for statistical computing. URL https://www.R-project.org/.

Rabaiotti, D. & Woodroffe, R. (2019). Coping with climate change: limited behavioral responses to hot weather in a tropical carnivore.*Oecologia* , 189, 587–599.

Refsnider, J.M. & Janzen, F.J. (2012). Behavioural plasticity may compensate for climate change in a long-lived reptile with temperature-dependent sex determination. *Biological Conservation* , 152, 90–95.

Sheridan, J.A. & Bickford, D. (2011). Shrinking body size as an ecological response to climate change. *Nature Climate Change* , 1, 401–406.

Sommer, S., van Benthem, K.J., Fontaneto, D. & Ozgul, A. (2017). Are generic early-warning signals reliable indicators of population collapse in rotifers? *Hydrobiologia* , 796, 111–120.

Stelzer, J.A.A., Mesman, J.P., Adrian, R. & Ibelings, B.W. (2021). Early warning signals of regime shifts for aquatic systems: Can experiments help to bridge the gap between theory and real-world application? *Ecological Complexity* , 47, 100944.

Stirling, I. & Derocher, A.E. (2012). Effects of climate warming on polar bears: a review of the evidence. *Global Change Biology* , 18, 2694–2706.

Strona, G. (2022). *Hidden Pathways to Extinction* . Fascinating Life Sciences. Springer International Publishing, Cham.

Su, H., Wang, R., Feng, Y., Li, Y., Li, Y., Chen, J., *et al.*(2021). Long-term empirical evidence, early warning signals and multiple drivers of regime shifts in a lake ecosystem. *Journal of Ecology* , 109, 3182–3194.

Uiterwaal, S.F., Lagerstrom, I.T., Luhring, T.M., Salsbery, M.E. & DeLong, J.P. (2020). Trade-offs between morphology and thermal niches mediate adaptation in response to competing selective pressures.*Ecol Evol* , 10, 1368–1377.

Venables, W.N. & Ripley, B.D. (2002). *Modern Applied Statistics with S* . Springer, New York, NY.

Vorobeichik, E.L. (2022). Natural Recovery of Terrestrial Ecosystems after the Cessation of Industrial Pollution: 1. A State-of-the-Art Review. *Russ J Ecol* , 53, 1–39.

Wikelski, M. & Cooke, S.J. (2006). Conservation physiology.*Trends in Ecology & Evolution* , 21, 38–46.

Wood, S.N. (2003). Thin Plate Regression Splines. *Journal of the Royal Statistical Society Series B: Statistical Methodology* , 65, 95–114.

Wood, S.N. (2011). Fast Stable Restricted Maximum Likelihood and Marginal Likelihood Estimation of Semiparametric Generalized Linear Models. *Journal of the Royal Statistical Society Series B: Statistical Methodology* , 73, 3–36.

Wood, S.N. (2017). *Generalized Additive Models: An Introduction with R, Second Edition* . CRC Press.

Supplementary Material

Supplementary Figures

Figure S1. Raw time series (column A) and detrended time series (column B) of the *Paramecium caudatum* mean swimming speed, mean body length and abundance of each replicate (N = 10) in the Control treatment.

Hosted file

`image4.emf` available at https://authorea.com/users/495424/articles/687702-multivariate-signals-of-population-collapse-in-a-high-throughput-ecological-experiment

Figure S2. Raw time series (column A) and detrended time series (column B) of the *Paramecium caudatum* mean swimming speed, mean body length and abundance of each replicate (N = 10) in the Pollution treatment. The red dashed line marks the beginning of the stressor (daily addition of a growing Cu^{2+} quantity).

Hosted file

`image5.emf` available at https://authorea.com/users/495424/articles/687702-multivariate-signals-of-population-collapse-in-a-high-throughput-ecological-experiment

Figure S3. Raw time series (column A) and detrended time series (column B) of the *Paramecium caudatum* mean swimming speed, mean body length and abundance of each replicate (N = 10) in the Predator treatment. The red dashed line marks the beginning of the stressor (arrival of 5 individuals of the predator flatworm *Stenostomum virginianum*).

Hosted file

`image6.emf` available at https://authorea.com/users/495424/articles/687702-multivariate-signals-of-population-collapse-in-a-high-throughput-ecological-experiment

Figure S4. GAMMSs predicted temporal trends (continuous lines) with 95% confidence interval (shaded areas) in EWSs metrics (coefficient of variation - CV, standard deviation - SD, and lag-1 autocorrelation - ACF) for abundance time series, comparing pollution vs control treatment (a) and predator vs control treatment (b). Note that the x axis (the temporal component) is normalised for each replicate using the time before collapse (time before experiment end for control treatments).